SUBCRITICAL CRACK GROWTH IN THREE ENGINEERING CERAMICS UNDER BIAXIAL CONDITIONS

L. Guerra Rosa*, J. Cruz Fernandes* and I. Alexandrino Duarte**

Three different materials - a reaction-bonded silicon carbide, a high-purity alumina, and a composite consisting of Al_2O_3 and 7 wt % ZrO_2 - are properly characterised in terms of microstructure and mechanical properties. The so-called "dynamic method" that consists of fracturing batches of specimens at different crosshead speeds in the testing machine is used to determine the Sub-Critical Crack Growth exponent *n*. Results obtained under biaxial flexure (using a self-aligning ring-on-ring jig) are presented. Comparison with results obtained under four-point uniaxial flexure is also made. Stress-volume effects, as well as friction and edge effects, are discussed.

INTRODUCTION

In ceramic materials, the phenomenon known as "static fatigue" has its origin in the growth of sub-critical cracks. It is generally accepted that the sub-critical crack growth rate, da/dt, depends on the stress intensity factor, K, and three regions can be identified in a da/dt *vs*. K plot. In Region I, the following equation is applicable:

$$\frac{da}{dt} = A\,K^{n} \qquad \text{................(1)}$$

where A and *n* are constants, typical of each material, but highly dependent on ambient media (1-5).

Since the time to final fracture, t_f, of a ceramic piece is essentially spent in Region I, we can estimate t_f using the relationship:

$$t_f = \int_{a_i}^{a_c} \left(\frac{1}{da/dt} \right) da \qquad \text{................(2)}$$

where a_i and a_c are, respectively, the initial and the final crack dimension.

* Department of Materials Engineering, I.S.T., 1096 Lisboa Codex, Portugal
** M.Sc. Student

Substituting equation 1 in equation 2 and integrating, we obtain:

$$t_f = 2\,(K_{Ii}^{2-n} - K_{Ic}^{2-n}) \,/\, [\sigma^2\, Y^2\, A\, (n-2)] \qquad \ldots\ldots\ldots\ldots\ldots(3)$$

where σ is the applied stress, $K_{Ii} = Y\,\sigma\sqrt{a_i}$, Y is a geometrical factor (that was assumed constant in the integration) and K_{Ic} is the fracture toughness of the material.

A detailed analysis of equation 3 shows that sub-critical crack growth (SCCG) only becomes relevant when the values of n are low. Materials with low tendency for SCCG have $n \geq 200$. Values of n between 50 and 200 indicate that the static fatigue phenomenon is already relevant. When the n-values are lower than 50, the time till final fracture of the ceramic piece (t_f) is relatively high, because the fracture process of the material is highly commanded by the SCCG mechanism (6). Since many ceramic materials do not reveal a static-fatigue threshold value of K, it should be mentioned that, when using SCCG sensitive materials in engineering applications, it is advisable to adopt large "safety factor"-values.

Several methods (7) can be used for the determination of n, allowing the comparison among different ceramics in what concerns to their sensitivity to the occurrence of SCCG. The so-called "dynamic method" is the most usual one and it consists in fracturing batches of specimens applying different crosshead speeds in the testing machine. According to previous works (7,8), we can calculate the value of n making use of the relationship:

$$\sigma_f = B\dot{\sigma}^{1/(n+1)} \qquad \ldots\ldots\ldots\ldots\ldots(4)$$

where σ_f is the mean value of the fracture stress results obtained in N specimens, B is a constant and $\dot{\sigma}$ is the stressing rate (which is related to the crosshead displacement rate, $\dot{\delta}$). In order to obtain reliable results of n through this method, it is necessary to use at least three crosshead speeds separated by one order of magnitude. Since the fracture stress results usually show a large scatter, the calculated values of n normally present an accuracy of between 10 and 25% (7).

MATERIALS AND TEST-PIECES PREPARATION

The materials used in this investigation were: *i)* high-purity alumina (Al_2O_3), *ii)* a composite made with 7 wt % ZrO_2 addition to Al_2O_3, and *iii)* a reaction-bonded silicon carbide (RB-SiC). Two types of test-pieces were used: parallelepipeds and disks.

The specimens of high-purity alumina and Al_2O_3 - 7 wt % ZrO_2 were prepared in the laboratory using commercially available powders (Alumina ALCOA CT3000SG and Zirconia Unitec Z-100). The parallelepipeds and the disks were obtained by unidirectional pressing of powder (22 MPa) followed by atmospheric sintering at 1600°C during 4 hours. The Al_2O_3 - 7 wt % ZrO_2 powder mixture was obtained by drying a water suspension of the two starting powders. To get a good homogenisation, this suspension was stirred for 1 hour in a ball mill. The test-pieces did not suffer any surface modification after sintering *i.e.* they were mechanically tested as-sintered. The final dimensions of the parallelepipeds were: b (width) = 3.5 mm, h (height) = 7.5 mm, and L (length) = 44 mm. The disks had a diameter d_o = 25 mm and thickness t = 2 mm.

The RB-SiC specimens were restricted to a batch of nominally identical disks with diameter d_o = 25 mm and thickness t = 3 mm. These SiC disks (Refel grade) were provided by Tenmat Ltd (Manchester, UK).

CHARACTERIZATION OF THE MATERIALS

Before carrying out the SCCG studies using flexure strength tests, the three materials were properly characterised in terms of density, grain size, Vickers hardness, Young modulus, and fracture toughness (see Table 1).

TABLE 1 - Microstructural characteristics and mechanical properties of the materials

	high-purity alumina	Al_2O_3 - 7 wt % ZrO_2	reaction-bonded SiC
density, [Mg/m^3] % of theoretical density	3.89 98.2%	3.98 98.2%	3.12 100%
volume % of free Silicon	-	-	21%
mean grain size, [μm] by the intersection method	5-6	5-6 (alumina phase)	6 (SiC grains)
Vickers hardness, [kgf/mm^2]	1671 HV5	1671 HV5	2041 HV1
Young modulus, [GPa] a) by the resonance method b) by ultrasonics	384 ± 6 a)	383 ± 4 a)	379 b)
fracture toughness, [$MPa\sqrt{m}$] by indentation method	3.6 ± 0.2	4.1 ± 0.2	3.6 ± 0.5

FLEXURE STRENGTH TESTS

Two types of flexure tests were conducted: *i)* four-point bend uniaxial flexural strength tests (using the test-pieces with parallelepiped geometry), and *ii)* ring-on-ring biaxial flexural strength tests (using the disks). All tests were carried out in an Instron electromechanical testing machine and the peak load at the instant of fracture (P_f) was recorded in each test.

Four-point bend uniaxial flexural strength tests

A fully articulated jig (with external span L_e = 40 mm and internal span L_i = 20 mm) was used and the 4-point bend uniaxial flexural strength results (σ_{f4}) were calculated through the equation:

$$\sigma_{f4} = \frac{3}{2} \frac{P_f (L_e - L_i)}{b\, h^2} \qquad \text{................(5)}$$

where P_f is the fracture load; b and h are the width and the height of the specimen, respectively.

Ring-on-ring biaxial flexural strength tests

For biaxial tests, a self-aligning ring-on-ring jig was used. The support ring diameter was 22.0 mm and the upper ring diameter was 7.6 mm. This type of test jig is similar in design to that shown by Godfrey (9) for three-ball support, and by Fessler and Fricker (10). The biaxial fracture strength was calculated (10) from the equation:

$$\sigma_{fb} = \frac{3P_f}{2\pi t^2}\left[(1+\nu)\ln\left(\frac{d_s}{d_u}\right)+(1-\nu)\left(\frac{d_s^2-d_u^2}{2d_o^2}\right)\right] \quad \ldots\ldots\ldots\ldots\ldots(6)$$

where P_f is the fracture load, t is the disk thickness, ν is Poisson's ratio (assumed 0.26 for the two alumina-base materials, and 0.24 for the RB-SiC), d_u, d_s and d_o are the upper ring, support ring and test-piece diameters respectively. To minimize the friction effects, we have used a rubber sheet (of thickness 0.6 mm and Shore hardness 60 ± 5) between the specimen and the support ring; and ordinary white Xerox copy paper (80 gm^{-2}) between the specimen and the upper ring.

Loading conditions and statistical analysis of results

In order to determine the SCCG exponent n, three crosshead displacement rates were used - 0.05 mm/min, 0.5 mm/min and 5.0 mm/min. - so that the "dynamic method" can be applied. All tests were performed in the ambient laboratory atmosphere at 21 ± 2 °C and relative humidity 40 ± 5 %. The number (N) of test-pieces used for each combination of test conditions (and material) is presented in Table 2. Figure 1 shows the log σ_f *vs.* log $\dot{\delta}$ plots for the three materials. The values of uniaxial flexure strength (σ_{f4}) and biaxial flexure strength (σ_{fb}) plotted in Figure 1 are the arithmetic mean of the fracture stress results obtained for each combination of test conditions.

TABLE 2 - Number (N) of test-pieces used for each combination of test conditions (and material). Values of Weibull Modulus (m) are also shown.

		Crosshead displacement velocity, $\dot{\delta}$ [mm/min] 0.05	0.5	5.0
high-purity alumina :				
	uniaxial	N=25 (m=10.9)	N=23 (m=10.4)	N=23 (m=10.3)
	biaxial	N=13	N=30 (m=11.1)	N=10
Al_2O_3 - 7 wt% ZrO_2 :				
	uniaxial	N=24 (m=16.8)	N=21 (m=15.0)	N=23 (m=16.4)
	biaxial	N=10	N=29 (m=12.5)	N=11
RB-SiC :				
	biaxial	N=6	N=11	N=6

Values of Weibull modulus (m) were calculated when the number of test results (N) was higher than 20 (11). In these cases, the two-parameter Weibull equation was applied and the experimental definition of the failure probability was done using the estimator (i - 0.5) / N, where i is the rank of the σ_f-value when all fracture stress results are positioned in increasing order.

DISCUSSION OF RESULTS

As it is seen from Figure 1, for the three materials, the mean values of σ_{f4} and σ_{fb} increase when the crosshead speed increases. This is explained by the fact that at lower strain rates there is more time for SCCG to occur.

For the two alumina-base materials, it is noticeable that the Weibull moduli obtained in the parallelepiped test-pieces (for uniaxial flexure) seem to be independent of the strain rate. Unfortunately, we did not get enough test-pieces with the disk geometry (for biaxial flexure) that could allow a reliable determination of Weibull modulus for all crosshead displacement rates. Despite this fact, the values of the Weibull modulus available for 0.5 mm/min crosshead rate in both materials, are not very different from the corresponding ones in the four-point bending test. Another important experimental evidence is that the mean values of σ_{fb} are higher than the corresponding mean values of σ_{f4}. The explanation for this fact can be found in two effects: *i)* influence of the edges on the parallelepiped test-pieces, *ii)* occurrence of friction between the disk test-pieces and the rings (12).

The assumption of the same distribution of defects is one of the premises in the deduction of equation 4. According to the results of Weibull modulus shown in Table 2, we can conclude that the distributions of defects are similar in all batches of the same material.

In the high-purity alumina, we got $n = 43$ in the four-point bending tests; and $n = 49$ in the ring-on-ring tests. The Al_2O_3 - 7 wt % ZrO_2 composite exhibited $n = 36$ in four-point bending and $n = 32$ in biaxial tests. Considering each material, the differences among the values of n obtained from the two types of loading are not relevant if the scatter typical of this kind of ceramics is taken into account. The Al_2O_3 - 7 wt % ZrO_2 composite has lower values of n probably due to the occurrence of microcracking prior to the test (associated with the expansion of zirconia particles). These microcracks might act as initiation sites for slow crack growth in the test-piece when the loading is applied.

CONCLUSION

This investigation has shown that these three engineering ceramics are sensitive to the occurrence of SCCG. In comparison with the high-purity alumina, the Al_2O_3 - 7 wt % ZrO_2 composite has more tendency to the occurrence of SCCG because it presents lower values of n.

The fact that the n-values, in uniaxial flexure and in equibiaxial flexure, are very similar (i.e. $n = 43 - 49$ for the high-purity alumina, $n = 32 - 36$ for the Al_2O_3 - 7 wt % ZrO_2 composite) reveals that the most adequate fracture criterion to be used in these two materials is probably the criterion of the maximum applied stress (13).

At room temperature, the mean values of flexural strength obtained in the high purity alumina, in uniaxial or in biaxial flexure, are slightly higher than the corresponding values obtained in the Al_2O_3 - 7 wt % ZrO_2 composite. The RB-SiC (with 21 vol % of free Si) presents much lower flexural strength.

REFERENCES

(1) S.M. Wiederhorn et al, J. Mater. Sci., Vol. 17, 1982, p. 3460.
(2) S.W. Freiman et al, J. Amer. Ceram. Soc., Vol. 62, 1979, p. 206.
(3) A.G. Evans, J. Mater. Sci., Vol. 7, 1972, p. 1137.
(4) S.M. Wiederhorn, J. Amer. Ceram. Soc., Vol. 50, 1967, p. 407.
(5) R.H. Dauskardt et al, J. Amer. Ceram. Soc., Vol. 73, 1990, p. 893.
(6) R. Morrell, "An Introduction for the Engineer and Designer", Her Majesty's Stationary Office, 1985.
(7) M.J. Reece and J.M. Cox, "Delayed Failure/Subcritical Crack Growth of Ceramics", National Physical Laboratory report DMM (A) 49, England, 1992.
(8) A.G. Evans and S.M. Wiederhorn, Int. J. Frac., Vol. 10, 1974, p. 309.
(9) D.J. Godfrey, Mater. Sci. Technol., Vol. 1, 1985, p. 510.
(10) H. Fessler and D. C. Fricker, J. Amer. Ceram. Soc., Vol. 67, 1984, p. 582.
(11) J.J. Fernandes et al, in "Proceedings of the 4th National Meeting of Sociedade Portuguesa de Materiais", edited by S.P.M., Lisbon, Vol. 1, 1989, p. 55.
(12) J.J. Fernandes and L. Guerra Rosa, in "Proceedings of the 5th National Meeting of Sociedade Portuguesa de Materiais", edited by A. P. Loureiro et al (S.P.M., Lisbon), Vol. 1, 1991, p. 375.
(13) J. J. FERNANDES, "Caracterização da Resistência à Fractura e Fadiga de Materiais Cerâmicos Estruturais", PhD Thesis, Tech. Univ. of Lisbon, 1994.

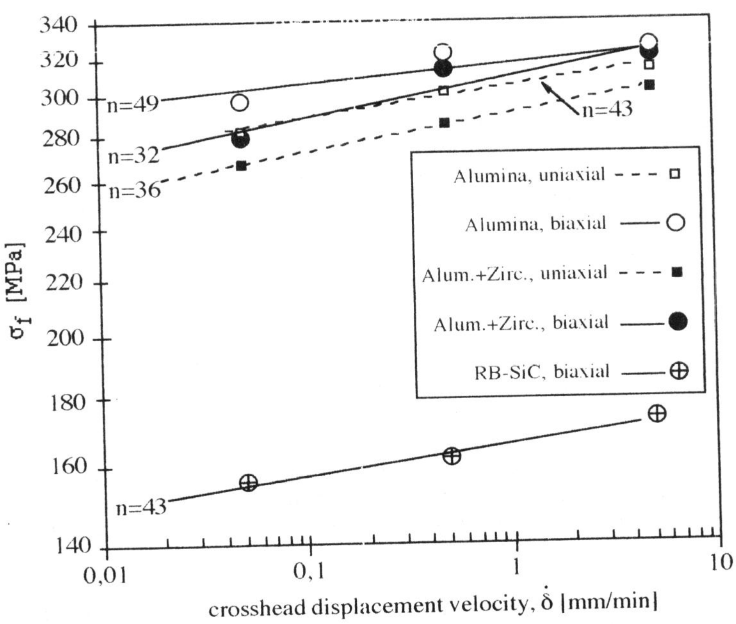

Figure 1 Log σ_f *versus* log $\dot{\delta}$ plots for the three materials.